



## MECHANICAL JOINT WITH HYSTERETIC DAMPERS AS BOLTED BEAM-TO-COLUMN MOMENT CONNECTION

Keiichiro SUITA<sup>1</sup>, Kazuo INOUE<sup>2</sup>, Ichiro TAKEUCHI<sup>3</sup> and Nobuyoshi UNO<sup>4</sup>

### SUMMARY

This paper presents an innovative structural system, named weld-free system, developed to overcome the difficulty in the quality assurance encountered in construction of steel moment resisting frames with conventional welded connections. The proposed structural system adopts a mechanical joint equipped with metallic-yielding damper as beam-to-column connection. An experimental verification of weld-free steel structures is presented. The test results clearly reveal the efficiency of the weld-free system in enhancing large and stable hysteresis loops while maintaining the beams and columns virtually in the elastic range until the ultimate state of the structure.

### INTRODUCTION

Among various types of structural materials, steel has long been the most popular in construction of commercial buildings in Japan with the vast majority of low-rise constructions. During the 1995 Hyogoken-Nanbu earthquake, a large number of steel buildings sustained severe damage or even collapsed, notably for two- to five-story structures (Nakashima et al. [1]; Reconnaissance[2]). One of the most serious damage appeared to be cracks and brittle fracture at welded beam-to-column connections. Similar to the observation from the 1994 Northridge earthquake (Youssef et al. [3]), the location where premature fractures initiated was typically in the vicinity of the weld between the beam bottom flange and the column flange.

To assure sufficient plastic deformation capacity of welded beam-to-column connections, several suggestions have been made in the U.S. and Japan. After extensive investigations, the reduced beam section design [4] has been widely accepted in the U.S. as an effective and economic solution. On the contrary, based on the observation that cracks often initiated at the toe of the weld access hole, Japanese researchers placed more emphasis on connection details to mitigate stress concentrations at welds and finally adopted the connection without weld access hole as an alternative for building construction [5]. Although these modified connections have shown satisfactory performance in laboratory, it is realized that

<sup>1</sup> Associate Professor, DPRI, Kyoto University, Kyoto, Japan. Email: suita@archi.kyoto-u.ac.jp

<sup>2</sup> Professor, Kyoto University, Kyoto, Japan. Email: inoue@archi.kyoto-u.ac.jp

<sup>3</sup> Senior Researcher, Nippon Steel Corporation, Chiba, Japan

<sup>4</sup> General Manager, Nippon Steel Corporation, Chiba, Japan

the quality of welds is difficult to control in practice as long as the structural fabrication relies on workmanship. A recent survey of experimental data of beam-column subassemblies [6] has confirmed some degree of uncertainty in the quality assurance of welds. Of 339 test specimens reviewed, 30 specimens exhibited premature fracture at welded metals as a result of weld defects. The defects as well as insufficient deposition are often of concern regardless of the connection details adopted. As compared to welded connections in the U.S., the Japanese practice generally requires larger volume of weld, implying that the Japanese connections are more relevant to the quality assurance problems (Nakashima [7]).

To overcome the difficulty in the weld quality assurance as well as stringent post-Kobe requirements for welding practice, an idea to mainly utilize bolts in beam-to-column connections with the number of welds minimized is appealing. In this regard, an innovative structural system, named ‘weld-free’ system, is proposed. The proposed system contains two distinctive features. First, with the wide-flange steel adopted for beams and columns, the conventional welded beam-to-column connection is replaced by a mechanical joint equipped with metallic-yielding damper. Second, super high-strength bolts recently developed are employed to reduce the number of bolts required and, in turn, use smaller cross-sections for the members being joined. The structural configuration and mechanical characteristics of the weld-free system are addressed in this paper. Furthermore, an experimental verification of weld-free steel structures is presented. Cyclic tests were conducted on three full-scale weld-free beam-column subassemblies and one base-line specimen with conventional post-Kobe welded connection. The test results are discussed with emphases on the energy dissipation and damage control efficiency.

## STRUCTURAL SYSTEM

### Structural Configuration

Fig. 1 shows the configuration of the proposed weld-free structural system. Wide-flange beams are bolted to the flanges of wide-flange column only at the top flanges as demonstrated in Fig 2. As a result, the beams rotate about the ends of their top flanges. At the top and bottom of the beam, braces are installed primarily to provide the structural system with sufficient lateral resistance against large design seismic force required in Japan and, at the same time, dissipate seismic input energy during a strong earthquake. For buildings with a large number of spans, conventional chevron braces can flexibly be arranged into some spans. However, the great majority of the Japanese construction involves small-scale structures having few spans. A more compact brace is, therefore, introduced to preserve large opening for normal usage [Fig. 2(a)]. In interior frames, large space is required and, thus, the brace may be implemented only at the bottom of the beam [Fig. 2(b)].

A brace of the buckling-restrained type is adopted. The buckling-restrained brace developed in this study is more compact than those devised previously (e.g., Watanabe [8]; Iwata et al. [9]). As shown in Fig. 3, the core plate is made of a steel rectangular bar coated by a friction-reduced material and encased in a restraining sheath made of steel tee section. The sheath can also be built from double steel flat plate whose performance has been verified by a more recent experimental investigation. Each end of the core plate is welded to an end plate which, in turn, is connected to the beam flange or column flange by high-strength bolts. Welding at the end plate is the only part in this system that requires highly skilled workmanship. To confine axial deformations of the buckling-restrained brace to the core plate, a small gap is provided between the restraining sheath and the end plate so that they do not contact each other when the brace sustains contractions.

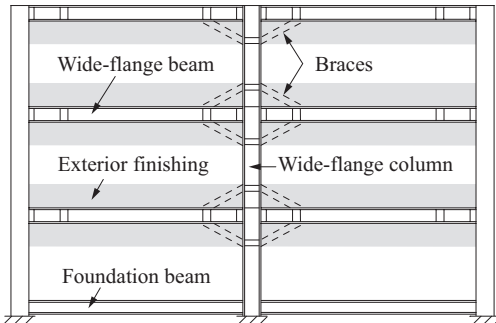
The weld-free structural system employs the connection between the beam top flange and the column flange as a mean for transferring gravity loads from the beams to the columns. The details of this connection will be introduced later. Under a strong ground motion, significant yielding excursion is expected only at the buckling-restrained braces. Beams and columns are designed to respond in the elastic

range, except at the base of the structure where some plastic deformations may be allowed in the columns. Accordingly, the behavior of the weld-free structural system can be regarded as ‘strong column-strong beam-weak brace.’

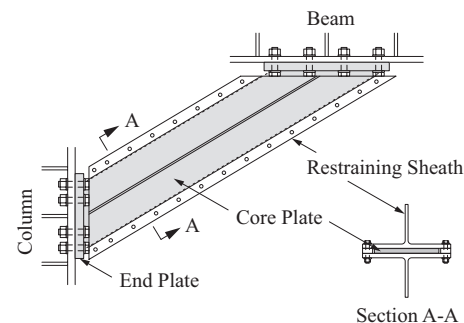
### Bending Moment Distribution

Fig. 4 presents the bending moment distribution in elastic beams and columns with weld-free connections (solid lines) in comparison to the case of conventional rigid welded connection (dashed line). The weld-free beam-column subassemblies are subjected to a lateral load which produces column shear force  $Q_c$  and beam shear force  $Q_b$ . Since the flexural stiffness of the brace is very low relative to the beam and column, pin connections are assumed between the beam and the column (point B) and between the brace and the extreme fibers of the beam or column (points A, C, D, and E). The beam has a half length  $l_b$  and a depth  $d_b$ , while a half story height  $l_c$  and a column depth  $d_c$  are assumed. The braces incline at an angle  $\alpha$  relative to the horizon. Their length is characterized by parameters  $\xi$  and  $\zeta$  as illustrated in the figure.

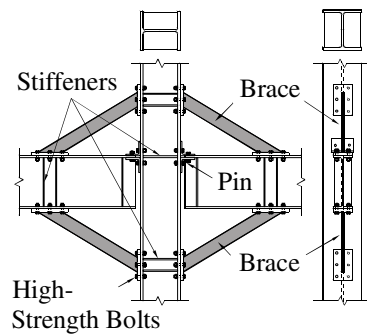
The moment distribution in beam is coincident in the cases of double- and single-side bracings. The weld-free connection is capable of carrying moment from the beam through a couple of forces exerted on the braces (also on the beam top flange-to-column flange connection for single-side bracing). This moment-carrying mechanism beneficially reduces bending moment in the beam and in some parts of the column, as compared to the moment distribution in the conventional system. The maximum bending moment in beam develops at point D with the magnitude of  $(1-\xi)l_bQ_b$ . The column moment reaches its peaks at the



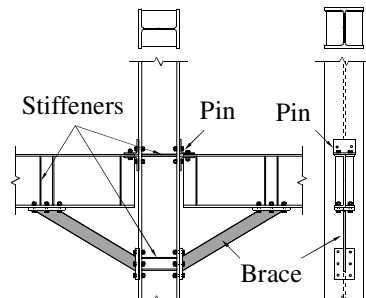
**Figure 1 Weld-Free Steel Building Structure**



**Figure 3 Details of Buckling-Restrained Brace**



**(a) Double-Side Bracing**



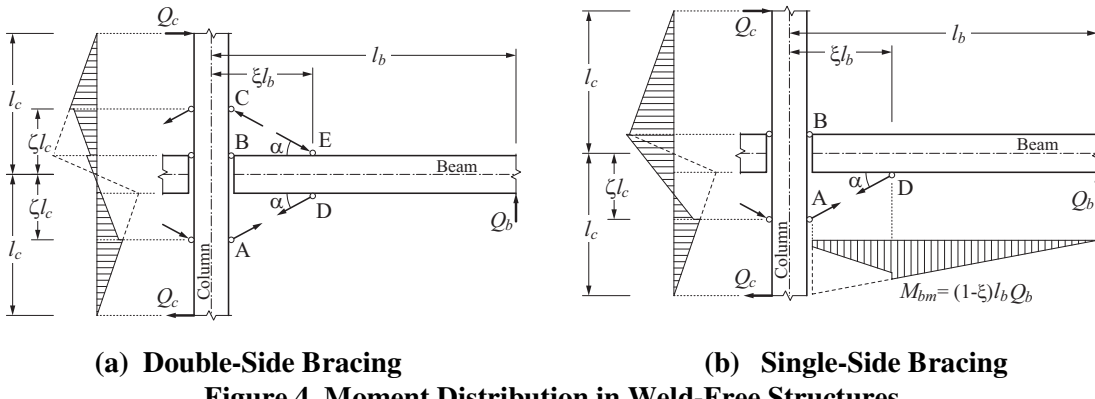
**(b) Single-Side Bracing**

**Figure 2 Details of Weld-Free Beam-to-Column Connections**

brace-column junctions. At these locations (points A, D), the discontinuity of bending moment is attributed to the eccentricity between the brace end and the centerline of the beam or column. Since the moment gradient in the column's panel is relatively low, shear force induced in the panel zone is reduced significantly. As such, the weld-free connection system does not require a web doubler plate to reinforce the panel zone. This advantageously allows flexible arrangement of beam-to-column connection details in the column's minor axis.

### Lateral Load-Carrying Mechanism

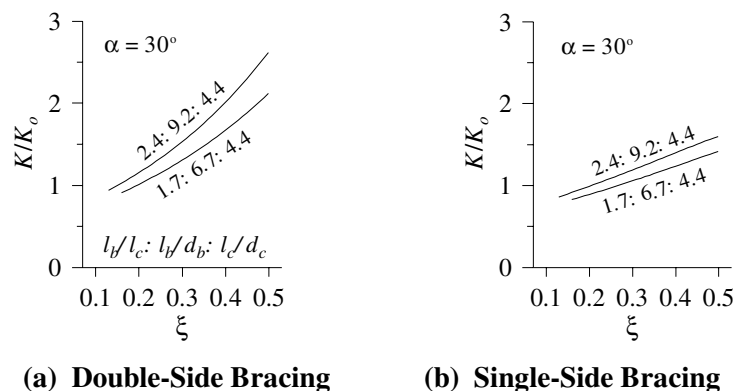
Weld-free steel frames possess high lateral stiffness due to the presence of buckling-restrained braces. Fig. 5 demonstrates the elastic lateral stiffness of weld-free beam-column subassemblies  $K$  normalized by the elastic lateral stiffness of conventional welded beam-column subassemblies  $K_o$ . The stiffness  $K$  is derived theoretically, assuming interior beam-column subassemblies with the braces inclined at 30 degree relative to the horizon. This brace inclination can appropriately be adopted in usual practice. The stiffness  $K_o$  is computed by considering flexural and shear deformations of the beams and columns as well as shear deformation of the panel zone. Two practical cases characterized by the ratios  $l_b/l_c : l_b/d_b : l_c/d_c$  are presented. In each case, the same beam and column cross-sections are used for all weld-free and conventional frames while the cross-sectional area of the braces is determined so that the lateral load-carrying capacity of the weld-free system is identical to that of the conventional system. It is notable that the lateral stiffness of weld-free systems is, in general, insensitive to the change in the axial stiffness of the brace. Fig. 5 clearly reveals that weld-free structures have the lateral stiffness comparable to the



(a) Double-Side Bracing

(b) Single-Side Bracing

Figure 4 Moment Distribution in Weld-Free Structures



(a) Double-Side Bracing

(b) Single-Side Bracing

Figure 5 Elastic Lateral Stiffness of Weld-Free Beam-Column Subassemblies

conventional frames when single-side bracing is adopted. The weld-free structures can be much stiffer if double-side bracing is implemented. The stiffness is greatly enhanced as the braced length of the beam (characterized by  $\xi$ ) increases and as the beams and columns become slender.

Presuming that all braces have the same yield force and exhibit elastic-perfectly plastic axial behavior, the lateral load-deformation relationship of weld-free systems is characterized by a bilinear or trilinear curve. For double-side bracing, axial deformation is larger at the bottom brace than the top brace since the center of the rotation at the beam end is located at the beam top flange (point B in Fig. 4). Yielding initiates first at the bottom brace followed by the top brace, leading to trilinear behavior. However, in all practical cases, the second yield force is very close to the first yield force and the behavior of weld-free systems with double-side bracing can be approximated reasonably by the bilinear load-deformation relationship. At the full plastic state, defined at yielding of the top and bottom braces, the theoretical beam shear force is expressed by

$$Q_{bp} = \frac{4\xi l_c}{2l_b - d_c} N_y \cos \alpha \quad (1)$$

where  $N_y$  = tensile yield force of the brace. The column shear force at the full plastic state can then be determined from  $Q_{bp}$ . For single-side bracing, the load-deformation relationship can be represented by a bilinear model. The beam shear force corresponding to yielding of the brace is computed by

$$Q_{bp} = \frac{2\xi l_c + d_b}{2l_b - d_c} N_y \cos \alpha \quad (2)$$

### **Super High-Strength Bolts for Compact Connections**

JIS F10T were the strongest high-strength bolts extensively used in Japan since the late 1970s. The minimum yield strength (0.2% offset) is 900 MPa, comparable to that of ASTM A490 bolts. Since the application of bolted connections is often limited due to an excessive number of bolts required, attempts have been made to enhance the yield strength of bolts. A newly invented super high-strength bolt, called F14T bolt, is a class of twist-off-type tension-control bolts. The configuration of F14T bolts is similar to standard bolts, except that the screw thread and the depth of the nut are modified to reduce stress concentrations under tension. The yield strength of, at least, 1260 MPa and the ultimate strength of 1400–1490 MPa are specified for F14T. For the same bolt diameter, F14T bolts would have the yield and ultimate forces of 1.46 times larger than F10T bolts because of the higher material strengths and larger effective cross-sectional area of the screw thread. The hydrogen embrittlement crack of F14T bolts has been prevented by reducing the stress concentrations as mentioned above and by chemically enhancing the capability of the bolt material to absorb a large amount of hydrogen without any exacerbation.

## **EXPERIMENTAL VERIFICATION OF WELD-FREE STEEL STRUCTURES**

### **Test Specimens**

The tests were aimed at verifying the cyclic performance of weld-free steel structures in comparison to a conventional welded moment resisting frame (MRF). A total of four full-scale models of beam-column subassemblies were fabricated. Two specimens are with double-side bracing, designated as D1 and D2, and one specimen is with single-side bracing, designated as S. The only difference between D1 and D2 is the cross-sectional area of the buckling-restrained brace, which was designed to achieve different ratios of the beam's moment demand to its flexural strength. The test results of D1 and D2 would suggest a suitable margin for the design flexural strength of the beam. In addition to the weld-free specimens, a conventional welded beam-column subassembly, designated as W, was constructed as a base-line specimen. Beams and columns of all specimens have the same lengths as shown in Fig. 6. The chosen cross-sections of the beams and columns were, respectively, wide-flange sections (depth × flange

width×web thickness×flange thickness in mm) of  $550\times200\times12\times22$  and  $414\times405\times18\times28$ . These cross-sections are typical of low- to medium-rise steel MRFs in Japan. Steel grades JIS SN400B and SN490B were selected for the beams and columns, respectively. For the buckling-restrain braces, the core plate was made of commercial low-yield strength (LYP) steel. Mechanical properties of steels obtained from coupon tests of sampled plates are summarized in Table 1.

#### *Specimens D1, D2, and S*

For all weld-free specimens, the braces are horizontally 1000 mm long and incline at 31 degree against the beam centerline. A rectangular bar of 16 mm thick was used as the core plate of the brace. Its width was selected so that the ratio of the maximum bending moment in the beam  $M_{bm}$  (equal to  $(1-\xi)l_bQ_{bp}$ ) to the beam yield moment  $M_{by}$  (computed by using material properties in Table 1 and the effective beam section to account for the loss of the cross-sectional area due to the bolt holes) is equal to 0.75, 0.92, and 0.83 for specimens D1, D2, and S, respectively. The obtained cross-sectional dimensions of the core plate and the resulting theoretical load-carrying capacities are listed in Table 2. It could be expected that the beams of specimens D1 and S would respond elastically until the ultimate state, since  $M_{bm}$  is limited fairly below  $M_{by}$ . On the other hand, with  $M_{bm}$  approximately equal to  $M_{by}$  the beams of specimen D2 might undergo beyond the proportional limit under large loading.

In the design of buckling-restrained braces, the maximum deformation was conservatively considered at the story drift angle of 0.02 rad which corresponds to two times of the story drift limit commonly considered in the building design against large earthquakes in Japan. The basic design criteria are that at this story drift: (1) yielding concentrates only in the braces while the beams and columns respond elastically; (2) based on observations of past experiments on buckling-restrained braces (e.g., Iwata et al.

**Table 1 Mechanical Properties of Steels Used for Test Specimens**

Steel Grade	Sampled Plates	Yield Strength (MPa)	Ultimate Strength (MPa)	Elongation (%)
SN400B	Beam flange	281	429	33
	Beam web	348	455	28
SN490B	Column flange	370	517	27
	Column web	370	508	29
LYP	Brace core	219	301	60

**Table 2 Dimensions of Braces and Resulting Load-Carrying Capacities of Beams**

Specimen	Dimensions of Brace Core Plate (mm)	$N_y$ (kN)	$Q_{cp}$ (kN)	$M_{bm}/M_{by}$
D1	$130\times15.5$	441	415	0.75
D2	$160\times15.5$	543	495	0.92
S	$220\times15.5$	747	447	0.83
W	—	—	566	—

[9]), axial strain in the core plate may properly be limited within 2% to ensure stable hysteresis behavior under a number of loading cycles; and (3) the restraining sheath remains elastic. The stiffness and strength required for the restraining sheath were determined based on a nonlinear analysis (Inoue et al. [10,11]). Fig. 7 presents the obtained design and connection details of each specimen. Frictions between the core plate and the restraining sheath were avoided by coating the core plate with molybdenum disulfide grease and providing a gap of 0.5 mm between the core plate and the restraining sheath [Fig. 7(d)]. The braces were fastened to the beam flange and column flange by F14T M22 super high-strength bolts through the end plates [Fig. 7(a) and (b)]. The end plates and the adjacent beam flange or column flange were

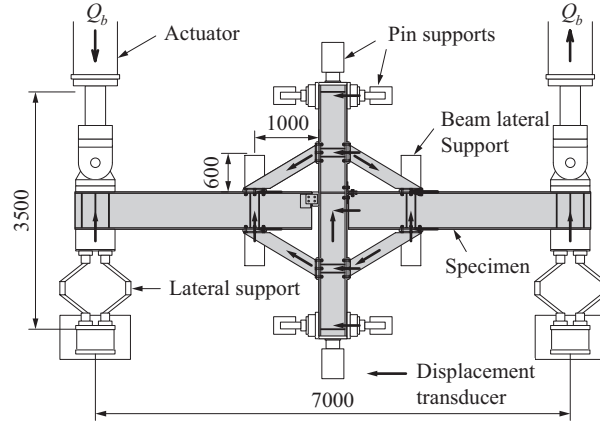


**Figure 6 Setup of Weld-Free Specimen and Instrumentation (Unit: mm)**

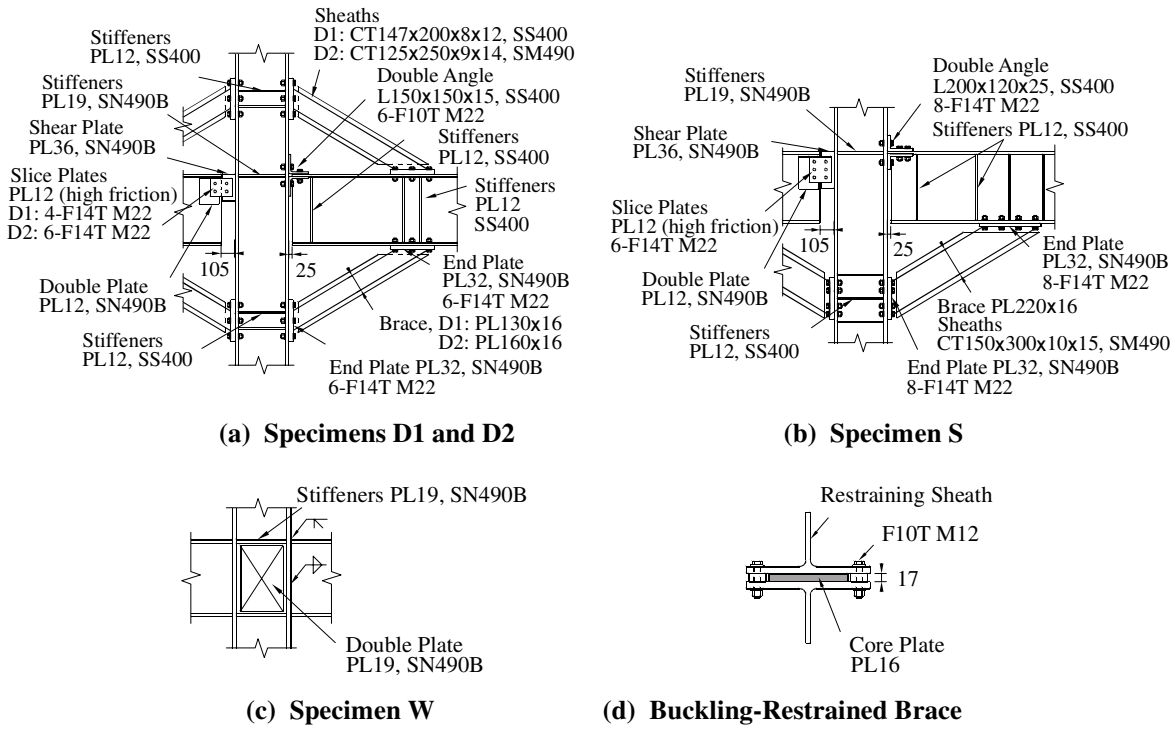


**Figure 7 Connection Details of Test Specimens (Unit: mm)**

designed so that, until the brace reached its tensile, they remained elastic and no significant slip or bolt prying occurred.

Although the connection between the beam top flange and column flange could be accomplished by double angle, the connection made by a shear plate fasten at the beam web in the vicinity of the beam top flange may be an alternative. In this regard, the right beam of each specimen was joined to the column by double angle connection while the joint at the left beam was made by a shear plate [Fig. 7(a) and (b)]. The double angle connection requires fillet-welded continuity plates to prevent out-of-plane deformations of the column flanges. On the contrary, the shear plate connection requires full penetration groove weld to attach the shear plate to the column flange. A clearance was provided between the beam and the column to prevent their contact even under the story drift angle of 0.04 rad.

#### *Specimen W*

Specimen W was fabricated in accordance with the post-Kobe practice [5,12]. The beams were shop-welded, without weld access holes, to the column by full penetration bevel welds at the beam flanges and two-sided fillet welds at the beam webs [Fig. 7(c)]. The column flanges were strengthened by continuity plates, and the panel zone was reinforced by a web double plate of 19 mm thick so that the panel zone remains elastic when the full plastic moment develops at the beam ends.

#### **Loading Setup and Program**

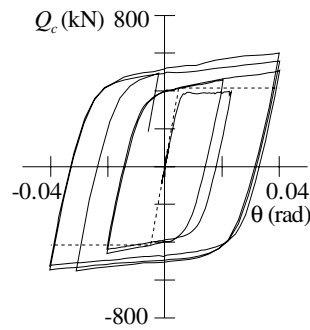
The test setup and locations of the displacement measurement relevant to the results discussed herein are as shown in Fig. 6. The column of each specimen was pinned at the tips to the reaction frame, and a hydraulic actuator was mounted to the end of each beam through a clevis. The cyclic story shear was applied quasi-statically to the specimen by means of transverse displacements at the beam tips. The two beams were simultaneously loaded in opposite directions based on an incremental load history containing two cycles of the story drift angle  $\theta = 0.02$  rad and subsequent cycles of  $\theta = 0.04$  rad applied until the ultimate state. In this study, the ultimate state is defined at which the maximum values of both positive and negative column shear forces are attained. It was expected that testing at the level of  $\theta = 0.02$  rad would reveal the performance of the structures under a large earthquake. Loading was, however, applied up to  $\theta = 0.04$  rad to explore the structural behavior under an extremely large earthquake.

#### **Test Results**

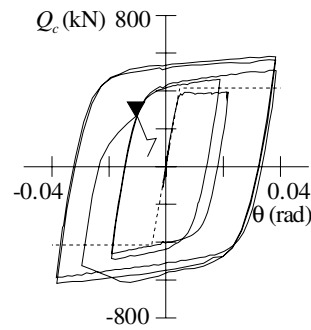
##### *Hysteresis Behavior*

Fig. 8 presents the column shear force  $Q_c$  (calculated by  $Q_b l_b / l_c$ ) versus story drift angle  $\theta$  relationship obtained from the left and right beams of each specimen. The positive sign refers to the loading direction depicted in Fig. 6. For comparison, the theoretical elastic lateral stiffness and the column shear forces at the full plastic state  $Q_{cp}$ , derived by means of (1) or (2) for the weld-free specimens and defined at the beam plastic moment for specimen W, are also plotted. For all weld-free specimens, the predicted initial slope of the load-deformation relationship virtually aligns with the experimental curve. The accuracy of the predicted column shear forces  $Q_{cp}$  is also notable. The discrepancy between the theoretical and test results of  $Q_{cp}$  is within 5%.

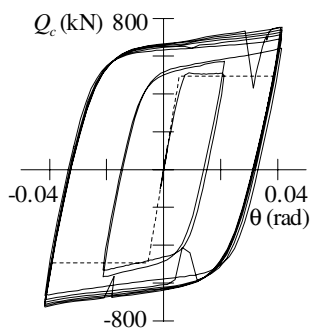
As observed in Fig. 8, all weld-free specimens exhibited stable hysteresis behavior until the ultimate state. The hysteresis loops of the right beams were larger than those of the left beams. This is due to the fact that using double angle to join the beam and column (right beam) would place the center of the beam end rotation right at the end of the top flange. On the contrary, the shear plate connection (left beam) located the rotation center at some distance below the beam top flange. The double angle connection, therefore,



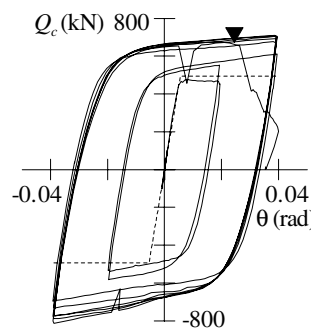
**(a) D1 Left Beam**



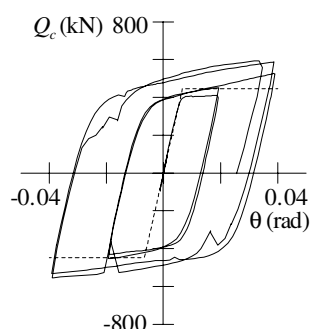
**(b) D1 Right Beam**



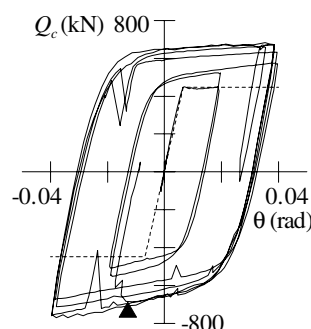
**(c) D2 Left Beam**



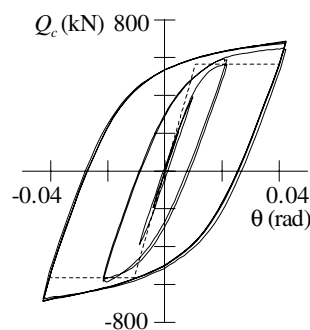
**(d) D2 Right Beam**



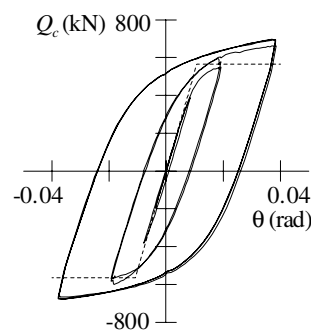
**(e) S Left Beam**



**(f) S Right Beam**



**(g) W Left Beam**



**(h) W Right Beam**

**Figure 8 Column Shear Force versus Story Drift Angle Relationship**

acquired larger moment arm of the bottom brace's yield force and, thus, greater lateral load-carrying capacity of the structural system

In 0.02 rad story drift cycles, specimens D1, D2, and S sustained plastic deformation only at the buckling-restrained braces without any signs of damage to other parts of the structures. The strain hardening engaged in the braces at 0.02 rad story drift amplitude caused an increase in the column shear force up to approximately 20%. This hardening should be taken into account in the design to prevent the beams and columns from unexpected plastic deformations. In 0.04 rad story drift cycles, slips occurred at the slip-critical joints in specimens D2 and S and caused an abrupt reduction in the load resistance [Fig. 8(c-f)]. The strength was, however, completely recovered thereafter.

Both specimens D1 and S suffered compression buckling at the core plate of the bottom-right buckling-restrained brace in the vicinity of the end plate, as a consequence of unexpected movement of the restraining sheath which expanded the unrestrained length of the core plate. The buckling occurred in cycles 5 and 7 for specimens D1 and S, respectively, and was followed by fracture at the location of the buckle at the instants marked in Fig. 8(b) and (f). Specimen S also sustained fracture of the super high-strength bolts at the shear plate connection of the left beam, suggesting that the arrangement of bolts at the shear plate should be reviewed to prevent large shear deformation caused by the beam rotation.

The movement of the restraining sheath was prevented in the test of specimen D2 by penetrating the sheath and the core plate through their thickness with a stud bolt at the mid length of the brace. Successful prevention of the brace buckling was evidenced by the test. This enabled specimen D2 to undergo a larger number of cycles under 0.04 rad story drift amplitude. In cycle 9, specimen D2 experienced fracture at the mid length of the core plate in the bottom-right brace and the energy was eventually exploited. The fracture occurred when the brace was loaded in tension at the instant marked in Fig. 8(d).

Unlike the nearly elasto-plastic behavior of the weld-free specimens acquired by uniform yielding in the braces, the behavior of specimen W was characterized by narrow hysteresis loops [Fig. 8(g) and (h)]. Its hysteresis behavior was associated with relatively low elastic stiffness and gradual decrease in the post-yield stiffness as a result of yielding progressed over the beam cross-section. Specimen W attained four cycles of 0.04 rad story drift amplitude before local buckling occurred at both top and bottom flanges of the left and right beams in the vicinity of the welded connection. The panel zone also experienced plastic shear deformation despite the presence of the web double plate. The test was terminated after some reduction in the load-carrying capacity indicating the achievement of the ultimate state.

#### *Energy Dissipation Behavior*

The amount of energy dissipated by the weld-free and conventional systems until the ultimate state is quantified in terms of the normalized cumulative plastic story drift angle  $\eta$ , defined as the ratio of the cumulative plastic story drift angle to the theoretical story drift angle at the full plastic state (equal to  $Q_{cp}/K$ ). The plastic story drift angle is cumulated as described in Fig. 9. Here, the results of the beams with the double angle connections are noted. The parameters  $\eta$  are 85, 152, and 84 for specimens D1, D2, and S, respectively. These values are substantially larger than that of specimen W where  $\eta$  is only 46. This comparison underlines the capability of weld-free systems to achieve greater energy dissipation at the ultimate state than the post-Kobe welded MRFs. It is worth noting that, unlike conventional welded MRFs, the energy dissipation and plasticity in the weld-free systems are concentrated only at the braces rather than the beams as will be shown later. These braces can be replaced after an earthquake with more ease than beams and columns.

### Plastic Deformation of Braces

Very stable hysteresis behavior was obtained at the buckling-restrained braces at the right beams as indicated by the column shear force  $Q_c$  versus brace axial strain  $\varepsilon$  relationship shown in Fig. 10. Here, the axial strain in the core plate is determined in an average sense by considering the measured elongation of the core plate. As expected, the bottom braces underwent larger deformation than did the top braces. To evaluate a degree of plasticity sustained by the buckling-restrained braces, the maximum axial strains of the core plate  $\varepsilon_m$  are summarized in Table 3. The strain  $\varepsilon_m$  is determined in the average sense by considering the measured elongation of the core plate. As expected, the bottom braces of all weld-free specimens underwent larger axial strains than did the top braces. The maximum axial strains of the bottom braces are found to be 3.0 to 3.5% at the applied story drift angle of 0.04 rad (before the cycles of fracture). At 0.02 rad story drift angle which was considered in the design of the braces, the maximum axial strains were approximately 50% smaller and fairly below the design strain limit of 2%.

Table 3 also presents the normalized cumulative plastic axial deformation  $\eta_d$  of the braces at the beams with double angle connections. The index  $\eta_d$  is defined as the ratio of the cumulative plastic axial deformation of the core plate (computed in a similar manner as illustrated in Fig. 9) to its yield axial displacement. The most notable value of  $\eta_d$  is observed at the bottom brace of specimen D2 where  $\eta_d$  is as high as 639. This result discloses the effectiveness of the developed buckling restraining system in preventing severe buckling of the core plate, leading to a large amount of the energy dissipation. The index  $\eta_d$  is significantly smaller for specimens D1 and S. However, provided that premature buckling of the braces was properly prevented, the deformation capacity of these two specimens should be increased considerably.

**Table 3 Summary of Deformations and Failure Mode of Braces at Beams with Double Angle Connections**

Specimen	Bracing Side	$\varepsilon_m$ (%)	$\eta_d$	Failure Mode
D1	Top	1.88	194	—
	Bottom	3.48	378	local buckling
D2	Top	1.65	331	—
	Bottom	3.28	639	tensile fracture
S	Bottom	3.03	495	local buckling

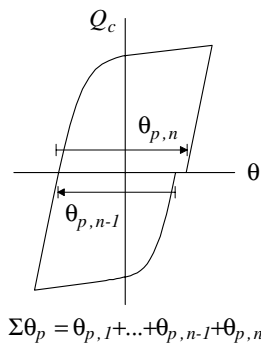


**Figure 9 Definition of Cumulative Plastic Story Drift Angle**

### *Plastic Deformation of Beams*

Control of damage in primary structural members is an important issue that reflects the efficiency of damage control systems. The damage to the test specimens is evaluated by means of plastic deformation sustained by the beams. Fig. 11 shows examples of the shear force-rotation relationship of the beams with double angle connections obtained from specimens D1 and D2. Here,  $\theta_b$  denotes the rotation of the unbraced beam portion, derived by dividing the relative transverse displacement between the beam tip and the beam-brace junction (caused by flexural and shear deformations of the beam) by the unbraced beam length. The plot clearly demonstrates essentially elastic response of specimen D1. The beam of specimen D2 experienced some yielding as a result of substantial strain hardening engaged in the braces. However, such plasticity is apparently insignificant. This observation suggests that weld-free structures can be designed by providing the beams with the yield moment equal to the maximum bending moment induced in the beams. Accordingly, plastic deformations will be concentrated only in the braces (possibly with slight yielding in the double angle connection) while the beams and columns respond nearly in the elastic range until the ultimate state of the structure.

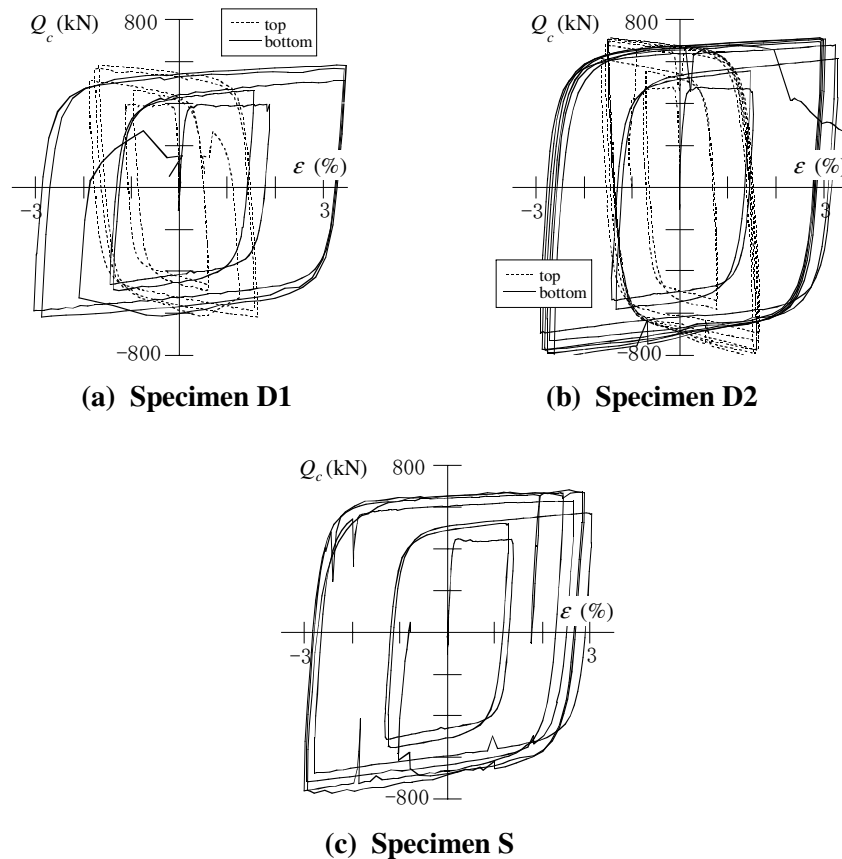


**Figure 10 Column Shear Force versus Brace Strain Relationship at Beams with Double Angle Connections**

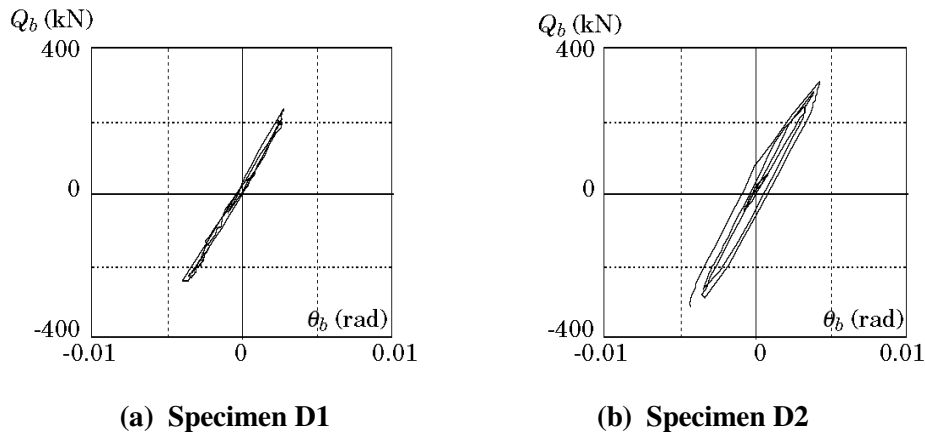


**Figure 11 Shear Force versus Rotation Relationship of Beams with Double Angle Connections**

## CONCLUSIONS

A novel structural system, named weld-free system, has been presented in this paper. This system was developed to overcome the quality assurance problem as well as stringent welding requirements. The experimental verification of weld-free structures has been conducted on three full-scale weld-free beam-column subassemblies and one specimen with conventional welded connection. It has disclosed that weld-free structures are capable of exhibiting stable hysteresis behavior under large story drift angles. Their hysteresis loops appear to be considerably larger than those of the conventional welded MRFs. The tests have shown a great advantage of weld-free structures in which plastic deformations can be limited only in the buckling-restrained braces while the beams and columns remain virtually elastic. It is recommended that double angle, rather than the shear plate connection, be used to connect the beam top flange and the column flange to ensure ductile behavior, large hysteresis loops, and high lateral resistance.

Although satisfactory performance of weld-free structures has been verified, extensive investigations need to be done to address crucial issues, including details of the beam-to-column connection in the column's minor axis, column base connection, and steel beam-reinforced concrete slab composite action.

## ACKNOWLEDGEMENT

The tests conducted in this study were supported by the Ministry of Education, Culture, Sports, Science, and Technology of Japan, Grant No. 12555159.

## REFERENCES

- 1 Nakashima, M., Inoue, K., and Tada, M. (1998). "Classification of damage to steel buildings observed in the 1995 Hyogoken-Nanbu earthquake." Eng. Struct., 20(4-6), 271-281.
- 2 Reconnaissance report on damage to steel building structures observed from the 1995 Hyogoken Nanbu earthquake. (1995). Kinki Branch, Architectural Institute of Japan, Osaka (in Japanese with attached abridged English version, M. Nakashima, ed.)

- 3 Youssef, N. F. G., Bonowitz, D., and Gross, J. L. (1995). "A survey of steel moment resisting frame buildings affected by the 1994 Northridge earthquake." NISTIR 5625, National Institute of Standards and Technology, Gaithersburg, MD.
- 4 Recommended seismic design criteria for new steel moment-frame buildings. (2000). FEMA350, Federal Emergency Management Agency, Washington, D.C.
- 5 Technical recommendations for steel construction for buildings. Part 1 Guide to steel-rib fabrications. (1996). Architectural Institute of Japan (in Japanese).
- 6 Report of survey and research on steelworks. (2000). Managing Committee of Structural Steelwork, Architectural Institute of Japan (in Japanese).
- 7 Nakashima, M. (2000). "Quality assurance for welding of Japanese welded beam-to-column connections." Procs. of Third Inter. Conf. on Behavior of Steel Struct. in Seismic Areas (STESSA 2000), Montreal, 223-230.
- 8 Watanabe, A., Hitomi, Y., Saeki, E., Wada, A., and Fujimoto, M. (1988). "Properties of brace encased in buckling-restraining concrete and steel tube." Proc., Ninth World Conf. on Earthquake Eng., Tokyo-Kyoto, IV, 719-724.
- 9 Iwata, M., Kato, T., and Wada, A. (2000). "Buckling-restrained braces as hysteretic dampers." Proc., Third Inter. Conf. on Behavior of Steel Struct. in Seismic Areas (STESSA 2000), Montreal, 33-38.
- 10 Inoue, K., Chang, P. Y., Mine, T., Hukuyama, K., and Inoue, K. (1993). "Stiffening design of the precast concrete panels to prevent the steel flat braces from buckling." J. Constr. Steel, Japan Society of Steel Construction, 1, 195-202 (in Japanese).
- 11 Inoue, K., Sawaizumi, S., and Higashibata, Y. (2001). "Stiffening requirements for unbonded braces encased in concrete panels." J. Struct. Eng., 127(6), 712-719.
- 12 Japanese Architectural Standard Specification: JASS 6 Steel Work. (1996). Architectural Institute of Japan (in Japanese).